Title	**Agent-based gateway operating system for RFID-enabled ubiquitous manufacturing enterprises**
Author(s)	**Fang, J; Huang, GQ**
Citation	**Robotics and Computer Integrated Manufacturing, 2013**
Issued Date	**2013**
URL	**http://hdl.handle.net/10722/189106**
Rights	**Creative Commons: Attribution 3.0 Hong Kong License**

Design and Analysis of a HTS Flux-Switching Machine for Wind Energy Conversion

Yubin Wang, Jianxin Sun, Zhixiang Zou, Zheng Wang, and K. T. Chau

***Abstract*—This paper proposes a new high-temperature superconductor (HTS) flux-switching machine with the merit of high power density for the direct-drive wind energy conversion system. The key is to introduce HTS windings to replace permanent magnet material in the flux-switching permanent magnet machine. Also, the use of HTS field excitation windings can easily achieve constant output armature voltage under time-varying wind speeds. By using the finite element analysis, the machine performances are analyzed. Hence, the validity of the proposed machine is verified.**

***Index Terms*—Finite element analysis, flux-switching machine, high-temperature superconductor, wind energy conversion.**

I. Introduction

As ONE of the fastest growing renewable energy source, wind energy has become globally attractive. In the last decades, various kinds of wind energy conversion (WEC) system have been proposed and exploited in sequence, namely the fixed-speed WEC system, variable-speed WEC system and PM direct-drive WEC system. Among of them, the fixed-speed and variable-speed WEC system can be named as the geared-drive WEC system due to the use of gearbox as the drive train component. This kind of system is dominant in the market at the present time since it possesses the merits of low cost and mature technology [1]–[3]. However, the gearbox inevitably suffers from many drawbacks such as frictional loss, regular maintenance and audible noise. Also, the slip rings and carbon brushes are generally employed to offer the rotor power which requires regular maintenance, resulting in machine failures and losses. For the PM direct-drive WEC system, although the gearbox, slip rings and carbon brushes are eliminated, its output armature voltage fluctuates with the random wind speed, which complicates the control of the grid-connected inverter. Moreover, since the PM direct-drive generator rotates at a low speed, the PM direct-drive WEC system has the drawbacks of bulky volume and heavy weight.

In recent years, the development of HTS machines provides an opportunity for the direct-drive WEC system having the merits of high power density and high efficiency [4]–[6]. In general, the HTS machines excited by field windings can be sorted into two categories, namely the rotor excitation and stator excitation according to the HTS field windings located in the rotor and stator, respectively. For the rotor excitation, the excitation current has to feed through slip rings and carbon brushes due to HTS field windings mounted in the rotor, which make the refrigeration complicated and difficult. In contrast, the stator excitation HTS machine allocates the HTS field windings in the stator. Hence, it is much easier for refrigeration than its rotor excitation counterpart.

In this paper, a new HTS flux-switching (HTS-FS) machine is proposed for the direct-drive WEC system. The proposed machine utilizes the BSCCO-2223 HTS tape as the field excitation windings which are mounted in the stator, hence attaining high power density and achieving flexible flux control to keep the amplitude of armature voltage constant under time-varying wind speeds. In Section II, the operation principle of the proposed machine will be discussed. Then, Section III will be devoted to using the FEA for machine performance analysis. Finally, conclusion will be drawn in Section IV.

II. Machine Configuration and Operation Principle

A. Machine Configuration

Fig. 1 shows the configurations of both of the FSPM machine and the proposed HTS-FS machine. The FSPM machine, which is shown in Fig. 1(a), consists of a rotor with 10 salient poles and a stator with 12 salient poles. The rotor is made of solid iron, without having any windings or PMs. The armature windings are set in the modular stator slots while the PMs are located between two stator modules to provide field excitation [7]. Borrowing from the idea of placing PMs in the stator to offer field excitation, the HTS field windings are employed to replace the PMs in the proposed HTS-FS machine as shown in Fig. 1(b). Hence, two kinds of windings, namely the copper armature windings and the HTS field windings, are arranged in the stator slots. It should be noted that the pole-pairs induced by the HTS field windings are the same as that of the PMs. Different from the conventional FS machine which uses copper windings to offer field excitation, the HTS-FS machine can provide much higher ampere-turns for the armature windings to significantly increase the machine power density.

Manuscript received September 28, 2012; accepted January 17, 2013. Date of publication January 22, 2013; date of current version April 12, 2013. This work was supported and funded in part by a grant (Project 51277183) from the National Natural Science Foundation of China, a grant (Project 2013CB035603) from the National Key Basic Research Program of China and a grant from the Fundamental Research Funds for the Central Universities (Project 12CX04058A) of China.

Y. Wang and J. Sun are with the College of Mechanical and Electrical Engineering, China University of Petroleum, Qingdao, China (e-mail: yubwang5190@163.com).

Z. Zou and Z. Wang are with the School of Electrical Engineering, Southeast University, Nanjing, China.

K. T. Chau is with the Department of Electrical and Electronic Engineering, The University of Hong Kong, Hong Kong, China.

Color versions of one or more of the figures in this paper are available online at http://ieeexplore.ieee.org.

Digital Object Identifier 10.1109/TASC.2013.2242113

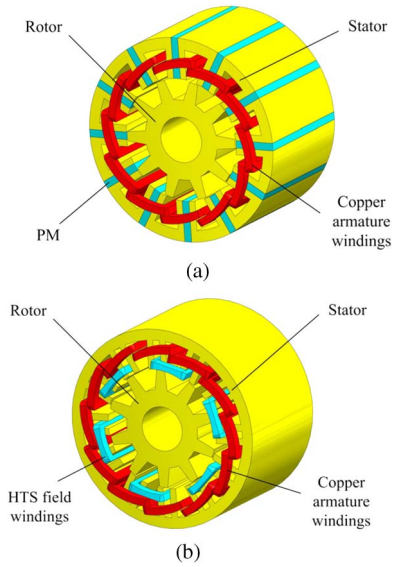

Fig. 1. Machine configuration: (a) FSPM machine and (b) proposed HTS-FS machine.

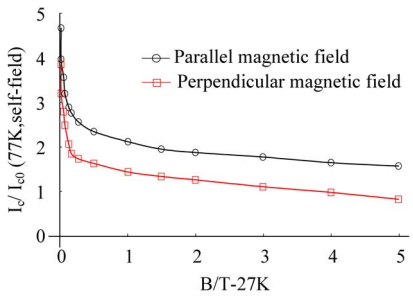

Fig. 2. Characteristic curve of current versus magnetic field of HTS field windings.

The critical current I_{c0} of BSCCO-2223 tape is about 100 A under self-field at 77 K. For the proposed machine, the operating temperature of the HTS field windings, which are wound as flat racetrack-coils, is around 27 K. So, a double-stage Gifford-Mcmahon cryocooler is employed to regulate the liquid nitrogen cooling system.

Fig. 2 depicts the characteristic curves of current versus magnetic field of HTS field windings under both the parallel magnetic field and the perpendicular magnetic field at the operating temperature. It can be found that the critical current I_c at 27 K is about 1.1 times that of the critical current I_{c0} at 77 K when the perpendicular magnetic field increases to 3 T. So, the rated current of field windings is set to 70 A to take into account the effect of magnetic saturation induced by self-field and armature reaction.

Compared with the FSPM machine, the proposed HTS-FS machine can offer some distinct advantages. Firstly, because of the HTS tape possessing the characteristic of high critical current density, the airgap flux density produced by HTS field windings is much higher than that of PMs. Consequently, the power density of the proposed machine can be increased significantly. Secondly, since the airgap flux density can be independently regulated by controlling the excitation current, the flexible magnetic flux control ability can be achieved. Thus, the armature back electromotive force (EMF) of the proposed machine can be kept constant under the time-varying wind speed. Thirdly, the proposed HTS-FS machine adopts the integrated stator yoke in such a way that the magnetic flux linked with armature windings can be increased effectively due to the decrease both of the magnetic reluctance and the leakage flux. Hence, the power density of the proposed machine can be further improved.

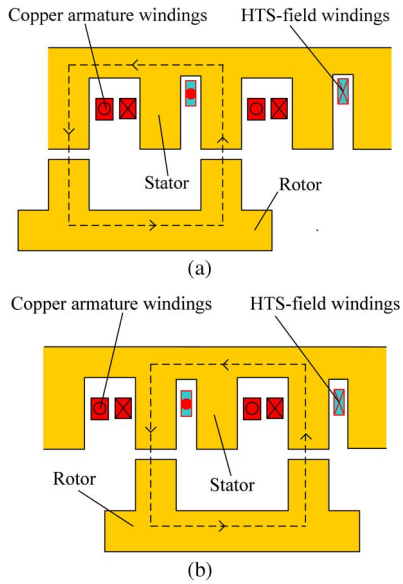

Fig. 3. Operation principle: (a) excitation flux approaching armature windings and (b) excitation flux leaving armature windings.

B. Operation Principle

Fig. 3 shows two special positions between the rotating rotor and the stationary stator, where the peak values of flux linkage can be obtained. According to the principle of minimum magnetic reluctance, when the rotor moves to the position as shown in Fig. 3(a), the excitation flux, which is excited by HTS field windings, approaches the armature windings via the airgap, and increases to the positive maximum value. On the contrary, when the rotor moves to the position as shown Fig. 3(b), the excitation flux leaves the armature windings, and decreases to the negative maximum value. Namely, the rotational movement through a rotor pole pitch causes 360° (electrical) change of EMF of the armature windings.

According to the operation principle of the HTS-FS machine, its pole-pair arrangement complies with the following criterion [8]:

$$N_s = 2mk \quad \text{and} \quad N_r = N_s \pm 2k \tag{1}$$

where N_s is the number of stator poles, N_r is the number of the rotor poles, m is the number of phases, and k is a positive integer.

III. Machine Analysis and Comparison

To verify the validity of the proposed machine, the performances are analyzed by using the FEA. In order to illustrate the advantages of the HTS windings, the proposed machine is quantitatively compared with a FSPM machine. The key design data of these two machines are summarized in Table I. It should be noted that the airgap length of the HTS-FS machine should

TABLE I
KEY DATA OF HTS-FS AND FSPM MACHINES

Parameters	HTS-FS	FSPM
Number of rotor poles	10	10
Number of stator poles	12	12
Stator outside diameter (m)	2.2	2.2
Stator inside diameter (m)	1.232	1.232
Rotor outside diameter (m)	1.22	1.212
Rotor inside diameter (m)	0.5	0.5
Stack length (m)	0.6	0.6
Airgap length (m)	0.006	0.008
Number of phases	3	3
Turns of armature windings per phase	2736	2736
Total turns of field windings	3900	/
HTS material	Bi-2223	/
PM material	/	Nd-Fe-B
PM volume (m^3)	/	0.0936

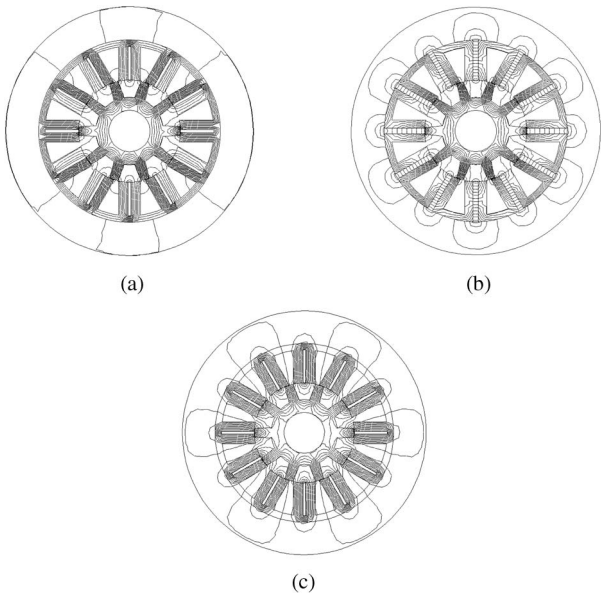

Fig. 4. No-load magnetic field distribution patterns: (a) HTS-FS machine with operating current of 70 A, (b) FSPM machine, and (c) HTS-FS machine with operating current of 100 A.

be set as short as possible subject to the physical constraint of assembly, whereas that of the FSPM machine is purposely set to 8 mm to avoid the possible irreversible demagnetization.

By using the FEA, the no-load magnetic field distribution patterns of the proposed HTS-FS machine with different operating current and the FSPM machine are shown in Fig. 4. As shown in Fig. 4(a) and (b), it can be seen that the flux leakage of the FSPM machine, namely outside the periphery of the stator, are much higher than that of the HTS-FS machine because the stator yoke of the FSPM machine is discontinuous. On the other hand, when the operating current of the HTS-FS machine is increased from 70 A to 100 A, the flux leakage becomes obvious because the magnetic circuit changes with the level of magnetic saturation of the stator yoke as shown in Fig. 4(a) and (c). Hence, the operating current and ampere-turns of the HTS field windings should be selected carefully to avoid magnetic saturation of the stator yoke.

Fig. 5 shows the magnetic field distribution around the BSCCO-2223 conductor. It can be found that since the stator core offers the magnetic paths for both the HTS magnetic field and the armature reaction field, the magnetic flux density that

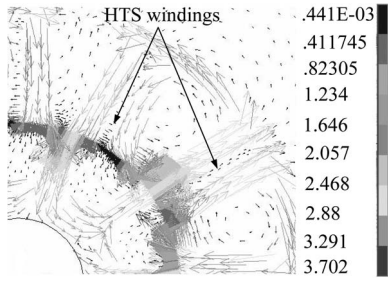

Fig. 5. Magnetic field distribution around the BSCCO-2223 conductor.

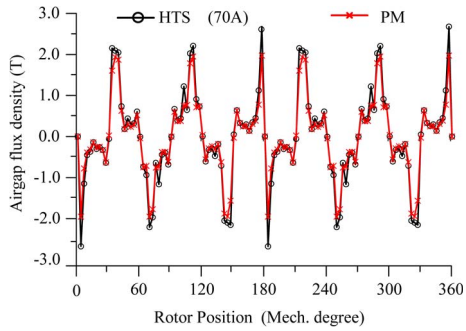

Fig. 6. Airgap flux density waveforms of HTS-FS and FSPM machines.

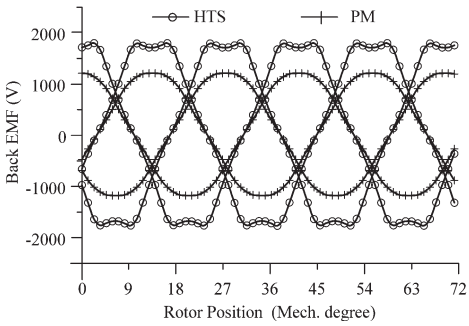

Fig. 7. Back EMF waveforms of HTS-FS and FSPM machines at speed of 5 rpm.

penetrates into the HTS conductor is very small. So, the AC losses caused by external magnetic fields can be suppressed effectively. In addition, the required cooling power for keeping the operating temperature is only a few hundred watts.

Fig. 6 depicts the no-load airgap flux density waveforms of both the HTS-FS machine with the operating current of 70 A and the FSPM machine. It can be seen that the maximum airgap flux densities of the HTS-FS machine and FSPM machine can reach 2.67 T and 1.97 T, respectively. Fig. 7 compares the no-load back EMF waveforms of these two machines at the speed of 5 rpm, which are deduced from the airgap flux density distributions. It can be found that the corresponding magnitudes of the HTS-FS machine and FSPM machine are 1785 V and 1196 V, respectively. It illustrates that the no-load EMF of the HTS-FS machine is 1.49 times that of the FSPM machine, which is consistent with the improvement in the airgap flux density and the decrease of the flux leakage. Consequently, the HTS-FS machine offers higher power density about 49% than that of FSPM machine under the same number of turns and diameter of conductors of the armature windings.

As discussed before, the high operating current of the HTS windings induces significant magnetic saturation in the stator

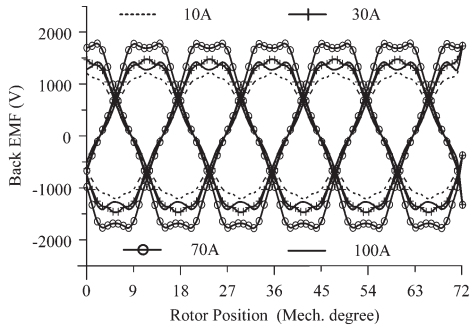

Fig. 8. No-load back EMF waveforms of HTS-FS machine with various operating currents.

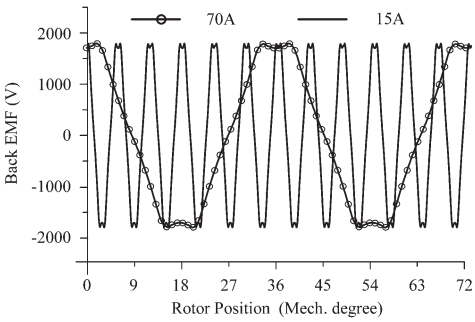

Fig. 9. Armature voltage waveforms of HTS-FS machine at speeds of 5 rpm and 30 rpm.

yoke and causes high flux leakage. Thus, its impact on the no-load back EMF should be investigated in particular. Fig. 8 shows the no-load back EMF waveforms of the proposed HTS-FS machine under various excitation current. It can be found that the operating current of 70 A is the optimal field excitation to maximize the no-load back EMF. When the operating current are lower than 70 A, the corresponding back EMF magnitudes increase with the values of operating current since the stator yoke does not reach magnetic saturation completely. In contrast, when the operating current is higher than 70 A, the magnetic reluctance of the stator yoke becomes very significant as the stator yoke is completely saturated. This can be observed in Fig. 4(c) that most of the flux pass through two adjacent stator teeth and form a closed path. This change of flux path leads to increase the flux leakage and hence decrease the back EMF as illustrated in Fig. 8. Consequently, the degree of magnetic saturation of the stator yoke can be regarded as one of the criteria for determining the number of turns of the HTS windings and the maximum value of the operating current.

For the direct-drive WEC system adopting the FSPM machine as a generator, the output armature voltage inevitably fluctuates with the random wind speed because its airgap flux density cannot be controlled flexibly. Since the field excitation current of the HTS-FS machine can be regulated independently, the WEC system employing the HTS-FS machine can keep the output armature voltage constant under time-varying wind speeds. This outstanding performance is confirmed by Fig. 9, in which the machine speed varies from 5 rpm to 30 rpm. It can be found that the magnitudes of no-load armature voltage are kept at 1785 V when the field current density is regulated from 70 A to 15 A.

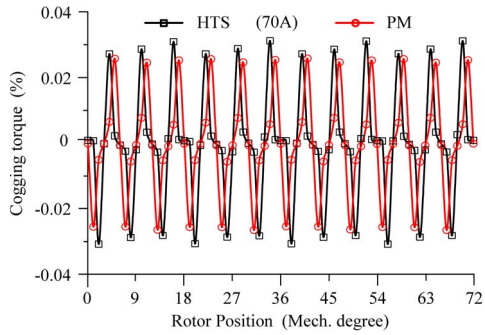

Fig. 10. Normalized cogging torque waveforms of HTS-FS and FSPM machines.

The cogging torque is an important parameter of PM machines to assess the retardation for initial rotor movement. For the proposed HTS-FS machine, its cogging torque can be considered as the retardation torque when the HTS windings are applied with the rated excitation current and the armature windings are open-circuited. Fig. 10 shows the normalized cogging torque waveforms of the two machines. It can be found that both of their values are lower than 0.04% which is very acceptable.

IV. Conclusion

In this paper, a new HTS-FS machine, adopting the HTS windings for field excitation, has been proposed for the WEC system. The machine configuration, operation principle, and design criteria have been discussed. By using the FEA, the proposed machine has been analyzed and quantitatively compared with the FSPM machine. It confirms that the proposed machine can offer the advantages of higher power density than its PM counterpart. Moreover, the HTS field excitation provides the flexibility to independently regulate the airgap flux so that the armature voltage can be kept constant under time-varying wind speeds. By assessing the machine performances, the validity of the proposed machine is verified.

References

[1] H. Polinder, F. F. A. van der Pijl, G.-J. de Vilder, and P. J. Tavner, "Comparison of direct-drive and geared generator concepts for wind turbines," *IEEE Trans. Energy Convers.*, vol. 21, no. 3, pp. 725–733, Sep. 2006.

[2] H. Li and Z. Chen, "Overview of different wind generator systems and their comparison," *IET Renew. Power Gen.*, vol. 2, no. 2, pp. 123–138, Jun. 2008.

[3] K. T. Chau, W. Li, and C. H. T. Lee, "Challenges and opportunities of electric machines for renewable energy," *Progr. Electromagn. Res. B*, vol. 42, pp. 45–74, 2012.

[4] A. B. Abrahamsen, N. Mijatovic, E. Seiler, M. P. Sorensen, M. Koch, P. B. Norgard, N. F. Pedersen, C. Traeholt, N. H. Andersen, and J. Ostergard, "Design study of 10 kW superconducting generator for wind turbine applications," *IEEE Trans. Appl. Supercond.*, vol. 19, no. 3, pp. 1678–1682, Jun. 2009.

[5] C. Liu, K. T. Chau, and W. Li, "Loss analysis of permanent magnet hybrid brushless machines with and without HTS field windings," *IEEE Trans. Appl. Supercond.*, vol. 20, no. 3, pp. 1077–1080, Jun. 2010.

[6] L. Jian, K. T. Chau, W. Li, and J. Li, "A novel coaxial magnetic gear using bulk HTS for industrial applications," *IEEE Trans. Appl. Supercond.*, vol. 20, no. 3, pp. 981–984, Jun. 2010.

[7] M. Cheng, W. Hua, J. Zhang, and W. Zhao, "Overview of stator-permanent magnet brushless machines," *IEEE Trans. Ind. Electron.*, vol. 58, no. 11, pp. 5087–5101, Nov. 2011.

[8] C. Liu, K. T. Chau, J. Zhong, and J. Li, "Design and analysis of a HTS brushless doubly-fed doubly-salient machine," *IEEE Trans. Appl. Supercond.*, vol. 21, no. 3, pp. 1119–1122, Jun. 2011.